Summary of lectures 1,2,3

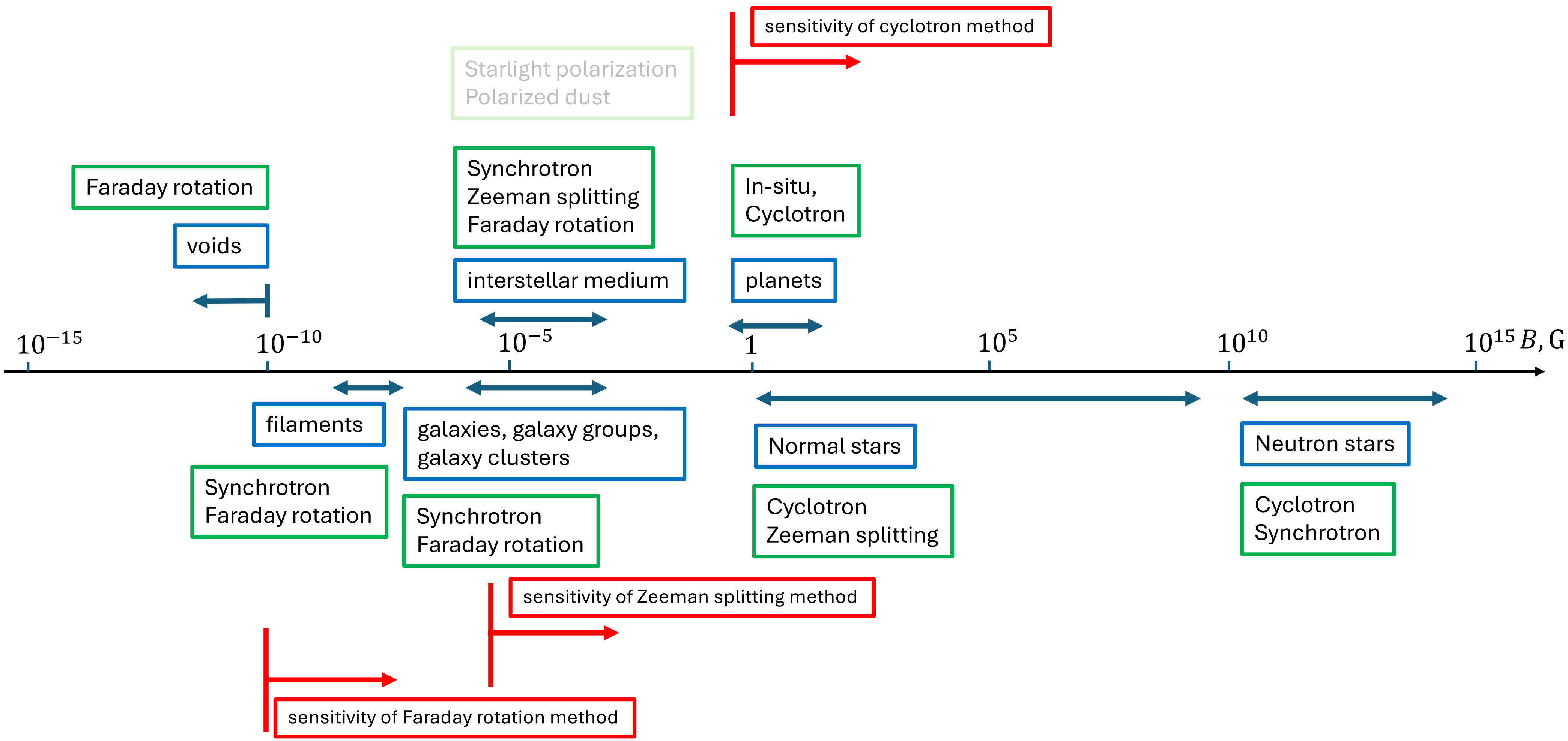

Cosmological magnetic field observations
Lecture 4
Magnetic fields across cosmic times

Ultra-high-energy cosmic ray (UHECR) constraint on magnetic field in void(s)

- UHECRobservations
- Deflections of UHECR by Galactic and intergalactic magnetic fields
- Constraint on IGMF in the local void

Gamma-ray measurements of magnetic field in cosmic voids

- Gamma-ray interactions in intergalactic medium
- Extragalactic Background Light
- Gamma-ray telescopes
- Extragalactic sources of TeV gamma-rays: blazars and gamma-ray bursts
- Lower bounds on IGMF from gamma-ray observations
- Prospects for measurements with new generation instruments: CTAO and LHAASO

Magnetic field evolution

- Largest processed eddies

Ultra-high-energy cosmic rays

Galactic magnetic field is responsible for diffusive escape of cosmic rays from the Milky Way disk and halo. Magnetic field in an object of the size R can retain charged particles as long as their gyroradius is much smaller than the object size

$$R_L = \frac{E}{eB} \ll R$$

$$E \ll eBR \simeq 10^{18} \left[\frac{B}{10^{-6}\ \mathrm{G}}\right] \left[\frac{R}{1\ \mathrm{kpc}}\right]\ \mathrm{eV}$$

Higher energy particles produced by Galactic sources would not be retained by the Milky Way magnetic field.

It is commonly assumed that the highest energy cosmic rays come from extragalactic sources. These highest energy particles are called Ultra-High-Energy Cosmic Rays. The energies of UHECR reach 10^{20} eV.

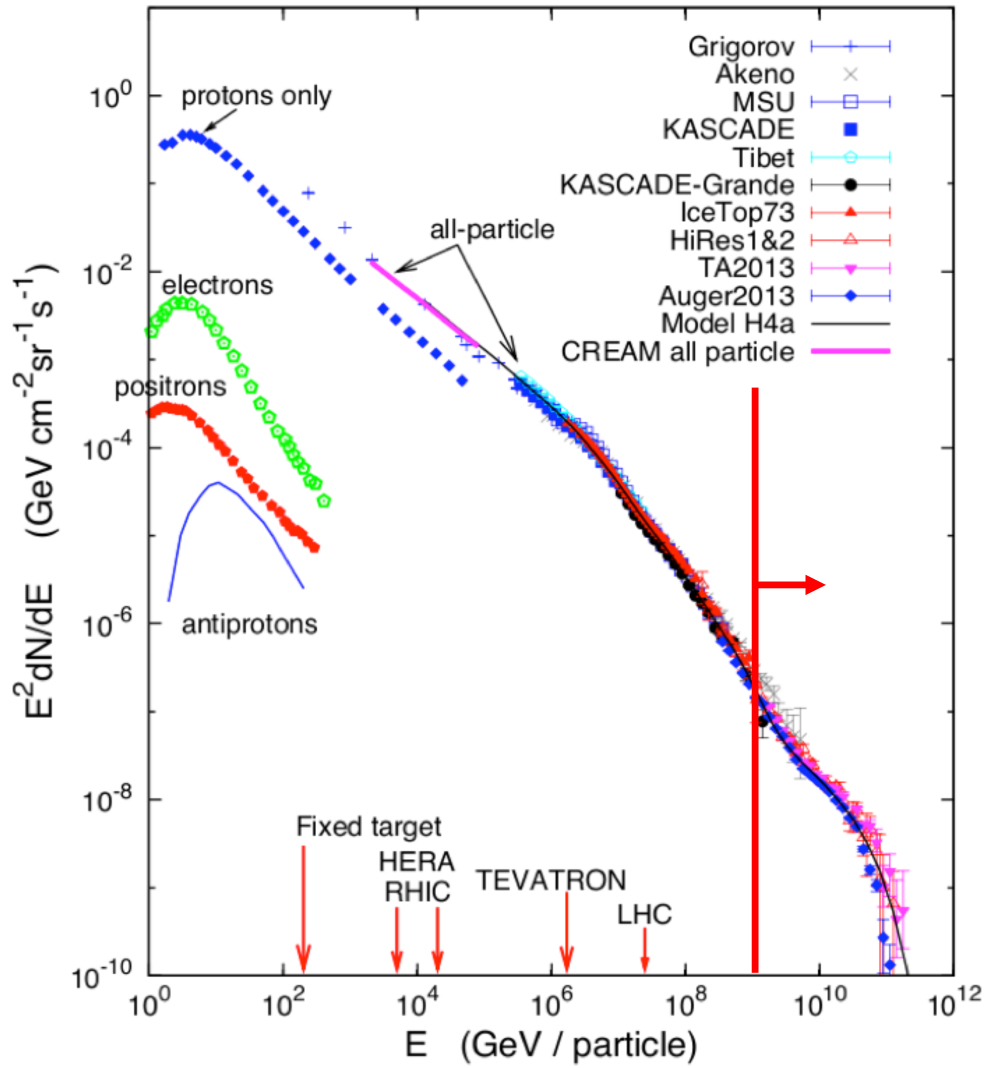

Ultra-high-energy cosmic rays

UHECR entering the atmosphere of Earth initiate Extensive Air Showers (EAS) of high-energy particles. The showers reach the ground level and can be detected by arrays of particles detectors scattered over large area.

High-energy particles moving in the atmosphere excite nitrogen molecules which produce blue fluorescence light. The EAS is visible as a "shooting star" during $\sim 10\ \mu s$ of its propagation though the atmosphere. This signal is detectable with fluorescence telescopes.

Pierre Auger Observatory (in Argentina) and Telescope Array (in US) are two UHECR experiments in Southern and Northern hemispheres.

Moderate expected deflections by the Galactic magnetic field motivate the idea of "UHECR astronomy": similar to photons, the arrival directons of UHECR are expected to point to their sources, it should be possible to observe UHECR sources on the sky.

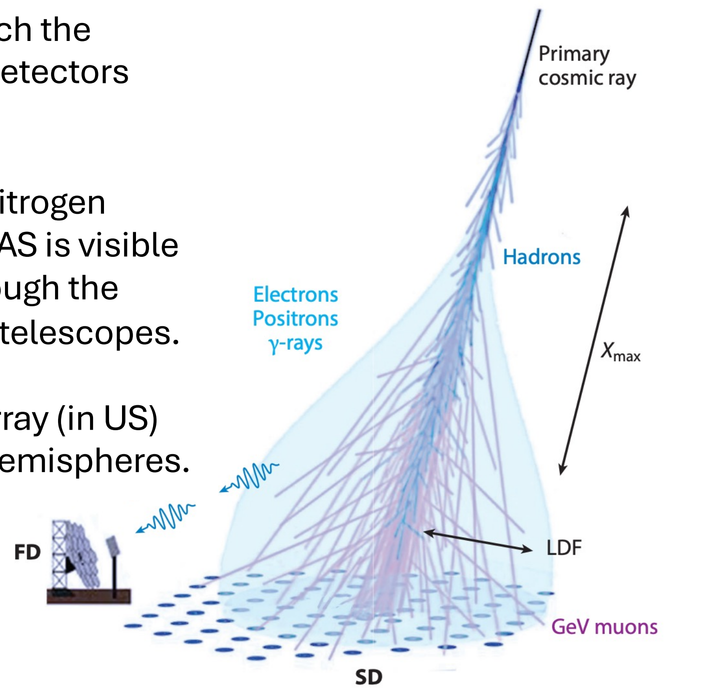

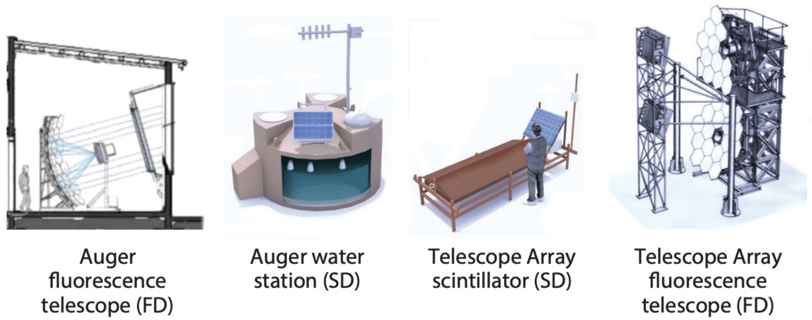

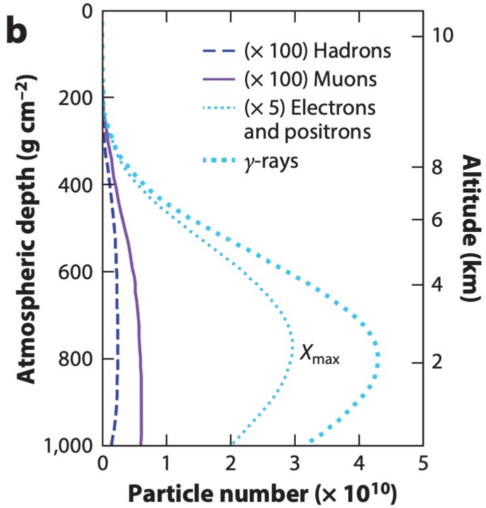

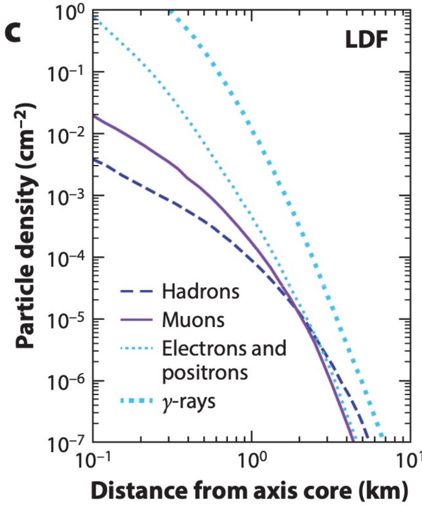

https://arxiv.org/abs/2505.21846

Ultra-high-energy cosmic rays

Gyroradius:

$$R_L = \frac{E}{ZeB} \simeq 100 \left[\frac{E}{10^{20}\ \mathrm{eV}}\right] \left[\frac{B}{10^{-6}\ \mathrm{G}}\right]^{-1} \mathrm{kpc}$$

where Z is the atomic number of the UHECR nucleus. Deflection angle of UHECR in Galactic magnetic field is

$$\theta_{GMF} = \frac{L}{R_L} \simeq 6^\circ Z \left[\frac{E}{10^{20}\ \mathrm{eV}}\right]^{-1} \left[\frac{B}{10^{-6}\ \mathrm{G}}\right] \left[\frac{L}{10\ \mathrm{kpc}}\right]$$

It is convenient to express the deflection angle in terms of rigidity $R = E/Z$

$$\theta_{GMF} = \frac{L}{R_L} \simeq 6^\circ \left[\frac{R}{10^{20}\ \mathrm{V}}\right]^{-1} \left[\frac{B}{10^{-6}\ \mathrm{G}}\right] \left[\frac{L}{10\ \mathrm{kpc}}\right]$$

Iron nucleus of energy 10^{20} eV has rigidity 3.8×10^{18} V. Proton of energy 10^{20} eV has rigidity 10^{20} V. Protons with energies 10^{20} eV are only moderately deflected by the Galactic magnetic field ($\theta_{GMF} \sim 1^\circ$) if their arrival directions are in Northern Galactic hemisphere (Galactic latitude $b > 0^\circ$), and moderate-to-large Galactic longitude. To the contrary, iron nuclei completely loose “memory” of their arrival direction when passing through the Galactic magnetic field.

Deflection map at 60 EV in JF12 model

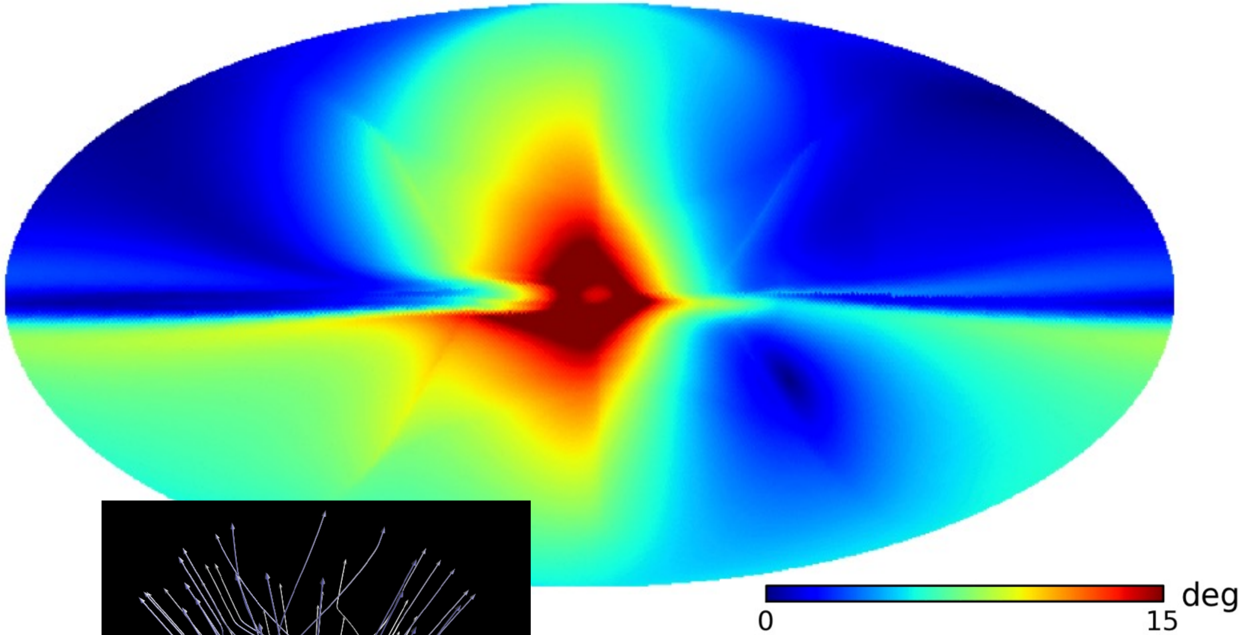

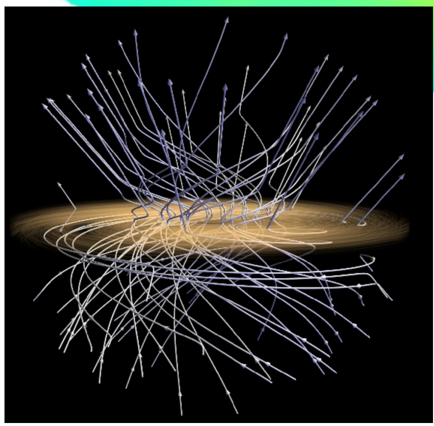

Deflections in intergalactic magnetic field (IGMF)

Gyroradius:

$$R_L = \frac{E}{ZeB} \simeq 100 \left[\frac{E}{10^{20}\ \mathrm{eV}}\right] \left[\frac{B}{10^{-6}\ \mathrm{G}}\right]^{-1} \mathrm{kpc}$$

where Z is the atomic number of the UHECR nucleus.
Deflection angle of UHECR in Galactic magnetic field is

$$\theta_{GMF} = \frac{L}{R_L} \simeq 6^\circ Z \left[\frac{E}{10^{20}\ \mathrm{eV}}\right]^{-1} \left[\frac{B}{10^{-6}\ \mathrm{G}}\right] \left[\frac{L}{10\ \mathrm{kpc}}\right]$$

It is convenient to express the deflection angle in terms of rigidity $R = E/Z$

$$\theta_{GMF} = \frac{L}{R_L} \simeq 6^\circ \left[\frac{R}{10^{20}\ \mathrm{V}}\right]^{-1} \left[\frac{B}{10^{-6}\ \mathrm{G}}\right] \left[\frac{L}{10\ \mathrm{kpc}}\right]$$

Iron nucleus of energy 10^{20} eV has rigidity 3.8×10^{18} V. Proton of energy 10^{20} eV has rigidity 10^{20} V. Protons with energies 10^{20} eV are only moderately deflected by the Galactic magnetic field ($\theta_{GMF} \sim 1^\circ$) if their arrival directions are in Northern Galactic hemisphere (Galactic latitude $b > 0^\circ$), and moderate-to-large Galactic longitude. To the contrary, iron nuclei completely loose "memory" of their arrival direction when passing through the Galactic magnetic field.

Gyroradius

$$R_L = \frac{E}{ZeB} \simeq 100 \left[\frac{E}{10^{20}\ \mathrm{eV}}\right] \left[\frac{B}{\mathbf{10^{-9}}\ \mathrm{G}}\right]^{-1} \mathbf{M}\mathrm{pc}$$

where Z is the atomic number of the UHECR nucleus.
Suppose there is a coherent magnetic field perpendicular to the line of sight over $L \sim 1 - 10$ **M**pc distance range. The deflection angle of UHECR is

$$\theta_{\boldsymbol{IGMF}} = \frac{L}{R_L} \simeq 6^\circ Z \left[\frac{E}{10^{20}\ \mathrm{eV}}\right]^{-1} \left[\frac{B}{\mathbf{10^{-9}}\ \mathrm{G}}\right] \left[\frac{L}{10\ \mathbf{M}\mathrm{pc}}\right]$$

Protons with energies 10^{20} eV are only moderately deflected by the IGMF with strength below 10^{-9} G.

If IGMF has correlation length much shorter than the distance to the source, IGMF deflections of different UHECR events would induce a scatter of UHECR arrival directions around the source (rather than displace the source position).

Ultra-high-energy cosmic rays

No firm source localisations and identifications have been achieved so far.

Observational data indicate that highest energy UHECR are intermediate mass nuclei, so that their deflections are larger and sources are more difficult to see.

Several “hotspots” (regions of enhanced UHECR flux) are observed on the sky). It is difficult to identify the sources of these hotspots:

- large uncertainties of the Galactic magnetic field model
- Large angular extent of the hotspots (~ 20°). Many astronomical sources are found within the hotspot extents.

Exercise 3. Explore Auger public dataset https://opendata.auger.org/ Build the skymap and spectrum starting from event lists.

https://arxiv.org/abs/2505.21846

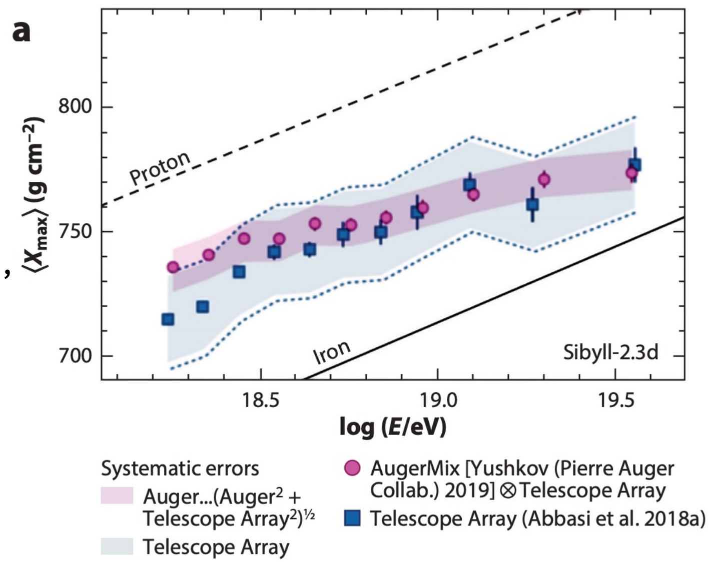

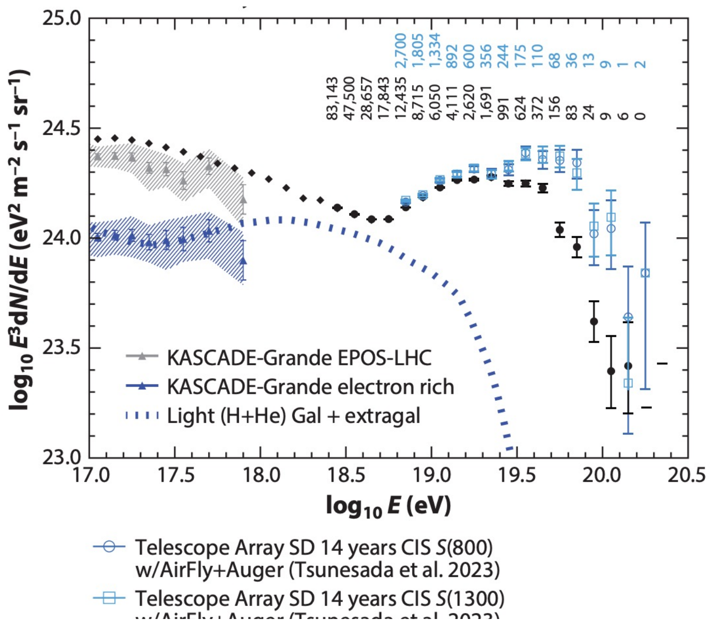

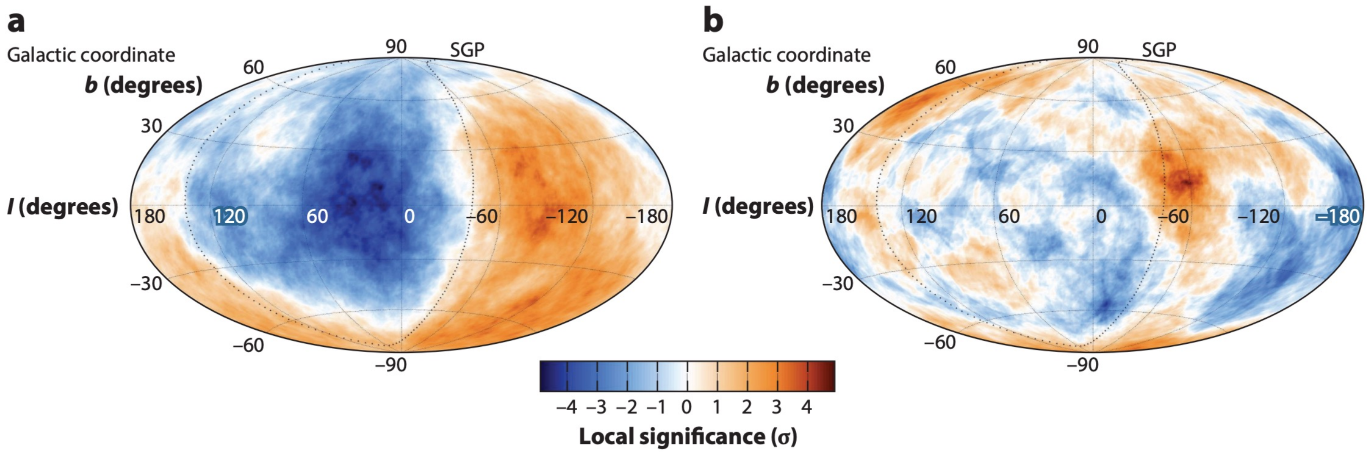

UHECR interactions in the intergalactic medium

UHECR particles interact on their way through their source, through interstellar medium of the host galaxy, through the intergalactic medium and through the Milky Way.

Consider e.g. head-on collisions with low energy photons (of CMB or Extragalactic Backgorund Light, EBL, the cumulative starlight from all galaxies). 4-momenta:

$$P_{uhecr} = (E, p, 0,0)$$
$$P_{ph} = (\epsilon, -\epsilon, 0,0)$$

Total 4-momentum $P_{tot} = P_{uhecr} + P_{ph}$, $P_{tot}^2 = -(E+\epsilon)^2 + (p-\epsilon)^2 = -m^2 - 2\epsilon(E+p)$.

At the energy threshold of e^+e^- pair produciton, the UHECR, the electron and positron are at rest in the center-of-mass frame, so that in this frame the total 4-momentum is $P_{tot,CM} = (m + 2m_e, 0,0,0)$, $P_{tot,CM}^2 = (m+2m_e)^2$. The square of the total 4-momentum is a scalar, $P_{tot} = P_{tot,CM}$, $\quad -m^2 - 2\epsilon(E+p) = -(m+2m_e)^2 = -m^2 - 4m_e(m+m_e)$. This gives

$$E_{thr,e^+e^-} \simeq \frac{m_e(m+m_e)}{\epsilon} \simeq 5\times 10^{17} \left[\frac{\epsilon}{10^{-3}\ \mathrm{eV}}\right]^{-1} \mathrm{eV}$$

In a similar way, the energy threshold of reaction producing pions, $p + \gamma \to p + \pi^0$, or $p + \gamma \to n + \pi^+$, is found from requirement that at the threshold the newly born pion is at rest, $P_{tot,CM} = (m + m_\pi, 0,0,0)$, $m_\pi \simeq 140\ \mathrm{MeV}$

$$E_{thr,\pi} \simeq \frac{m_\pi(m + m_\pi/2)}{2\epsilon} \simeq 7\times 10^{19} \left[\frac{\epsilon}{10^{-3}\ \mathrm{eV}}\right]^{-1} \mathrm{eV}$$

Interactions with photon backgrounds lead to energy loss of UHECR on distance scales

$$D_{uhecr} = \frac{1}{\kappa \sigma n_{ph}}$$

where σ is the interaction cross-section (e.g. of e^+e^- pair production, of pion production etc) and κ is the average inelasticity of collisions.

UHECR interactions in the intergalactic medium

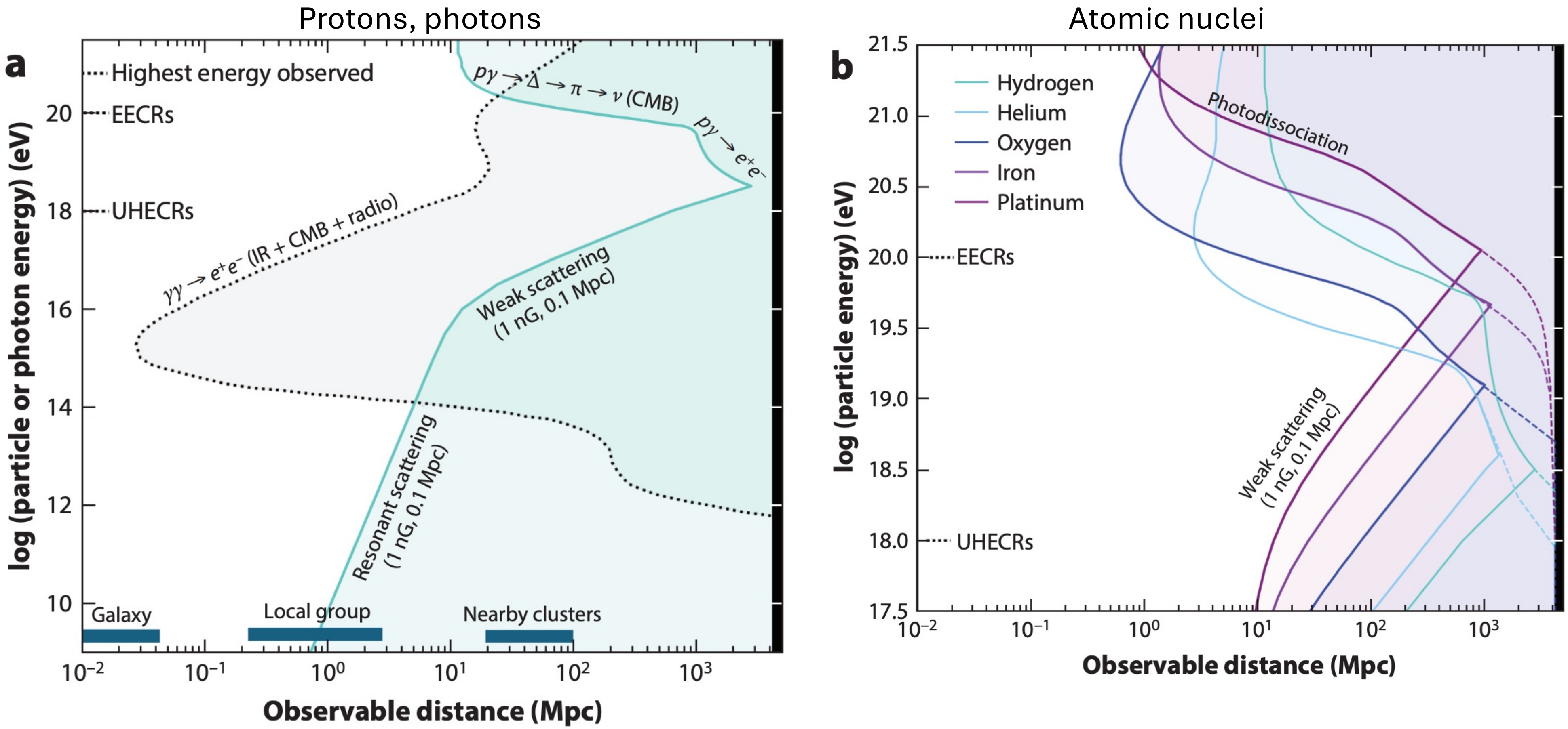

Sources of UHECR should be in "nearby" Universe. UHECR interact with CMB and with Cosmic Infared Background photons, via e^+e^- pair produciton and pion production. Atomic nuclei also photo-disintegrate. This limits the distance to UHECR sources to below ~ 100 Mpc.

https://arxiv.org/abs/2505.21846

Ultra-high-energy cosmic ray sources

UHECR sources are not identified, but among the sources behind the "hotspots", sources of interest are those that can retain the UHECR particles long enough to enable an acceleration mechanism to work. The necessary condition of UHECR retention is srong enough magnetic field in the source (of the size R):

$$R_L = \frac{E}{eB} \ll R$$

$$B \gg \frac{E}{eR} \simeq 10^{-4} \left[\frac{E}{10^{20}\ \mathrm{eV}}\right] \left[\frac{R}{1\ \mathrm{kpc}}\right] \mathrm{G}$$

Nearby starburst galaxies, galaxy clusters and active galactic nuclei can be or host UHECR sources.

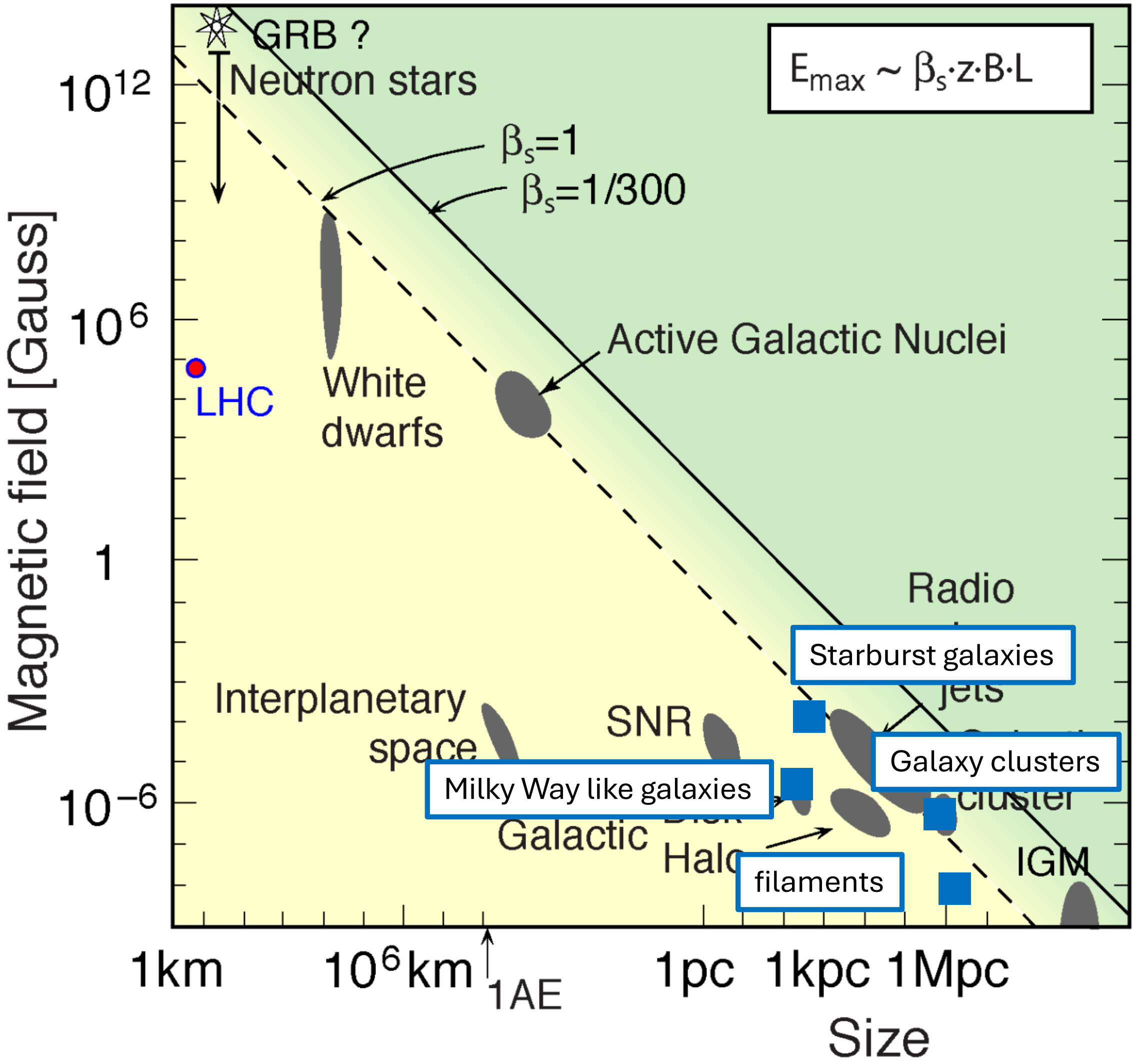

Constraint on void magnetic field from UHECR

One of UHECR hotspots observed by Telescope Array experiment is in the direction of Perseus-Pisces supercluster, behind the Local Void. The cluster is at $D \simeq 70$ Mpc distance. Deflections of UHECR by magnetic field in the Local Void:

$$\theta_{IGMF} = \frac{eBD}{E} \simeq 15^\circ \left[\frac{B}{10^{-10}\ \mathrm{G}}\right]\left[\frac{E}{2.5\times10^{19}\ \mathrm{eV}}\right]^{-1}\left[\frac{D}{70\ \mathrm{Mpc}}\right]$$

(2.5×10^{19} eV is the threshold of Telescope Array data analysis).

Mere existence of the hotspot limits the strength of magnetic field in the local void: too strong field would deflect UHECR particles away from direction toward the Earth.

If magnetic field in the Local void is variable on distance scale $\tilde{\lambda} < D$, the deflection within one field coherence scale is $\delta\theta = eB\tilde{\lambda}/E$. The deflections in subsequent coherence scale size cells are not correlated so tha the overall deflection angle grows as square root of the number of coherent cells along the line of sight, $N = D/\tilde{\lambda}$

$$\theta_{IGMF} = \sqrt{N}\frac{eB\tilde{\lambda}}{E}$$

$$\simeq 15^\circ \left[\frac{B}{10^{-10}\ \mathrm{G}}\right]\left[\frac{E}{2.5\times10^{19}\ \mathrm{eV}}\right]^{-1}\left[\frac{D}{70\ \mathrm{Mpc}}\right]^{\frac{1}{2}}\left[\frac{\tilde{\lambda}}{70\ \mathrm{Mpc}}\right]^{\frac{1}{2}}$$

The limit on B worsens with decreasing $\tilde{\lambda}$ as $\tilde{\lambda}^{-1/2}$.

https://arxiv.org/pdf/2510.02739

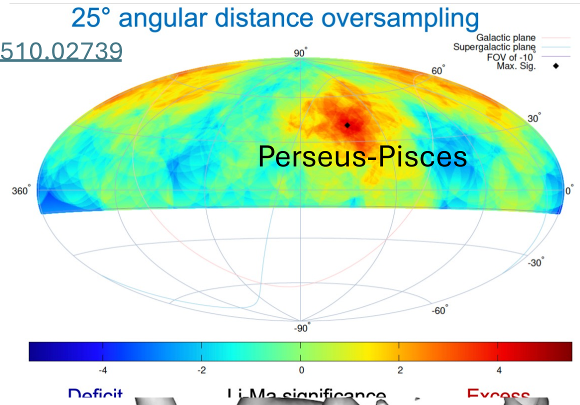

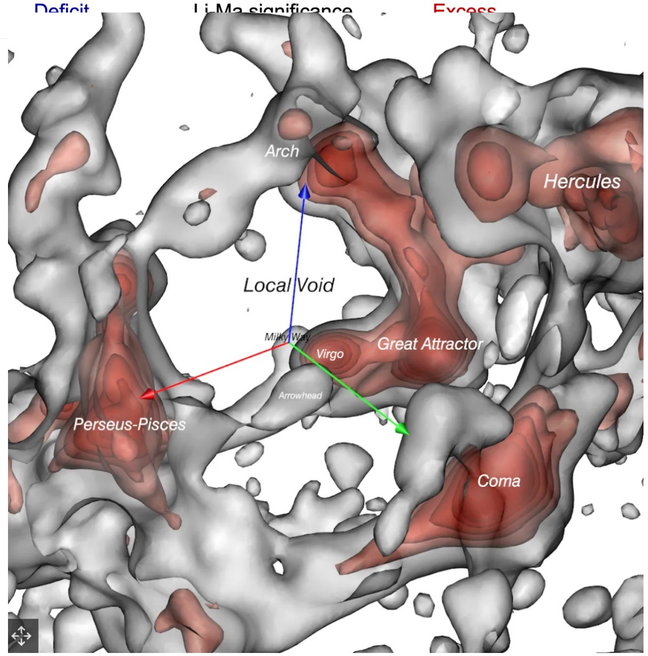

A rendition of the area surrounding the Local Void, with our galaxy at the center of the three arrows. (Image credit: R. Brent Tully)

…3202

Constraint on void magnetic field from UHECR

One of UHECR hotspots observed by Telescope Array experiment is in the direction of Perseus-Pisces supercluster, behind the Local Void. The cluster is at $D \simeq 70$ Mpc distance. Deflections of UHECR by magnetic field in the Local Void:

$$\theta_{IGMF} = \frac{eBD}{E} \simeq 15^\circ \left[\frac{B}{10^{-10}\ \mathrm{G}}\right] \left[\frac{E}{2.5\times10^{19}\ \mathrm{eV}}\right]^{-1} \left[\frac{D}{70\ \mathrm{Mpc}}\right]$$

(2.5×10^{19} eV is the threshold of Telescope Array data analysis).

Mere existence of the hotspot limits the strength of magnetic field in the local void: too strong field would deflect UHECR particles away from direction toward the Earth.

If magnetic field in the Local void is variable on distance scale $\tilde{\lambda} < D$, the deflection within one field coherence scale is $\delta\theta = eB\tilde{\lambda}/E$. The deflections in subsequent coherence scale size cells are not correlated so tha the overall deflection angle grows as square root of the number of coherent cells along the line of sight, $N = D/\tilde{\lambda}$

$$\theta_{IGMF} = \sqrt{N}\frac{eB\tilde{\lambda}}{E}$$

$$\simeq 15^\circ \left[\frac{B}{10^{-10}\ \mathrm{G}}\right] \left[\frac{E}{2.5\times10^{19}\ \mathrm{eV}}\right]^{-1} \left[\frac{D}{70\ \mathrm{Mpc}}\right]^{\frac{1}{2}} \left[\frac{\tilde{\lambda}}{70\ \mathrm{Mpc}}\right]^{\frac{1}{2}}$$

The limit on B worsens with decreasing $\tilde{\lambda}$ as $\tilde{\lambda}^{-1/2}$.

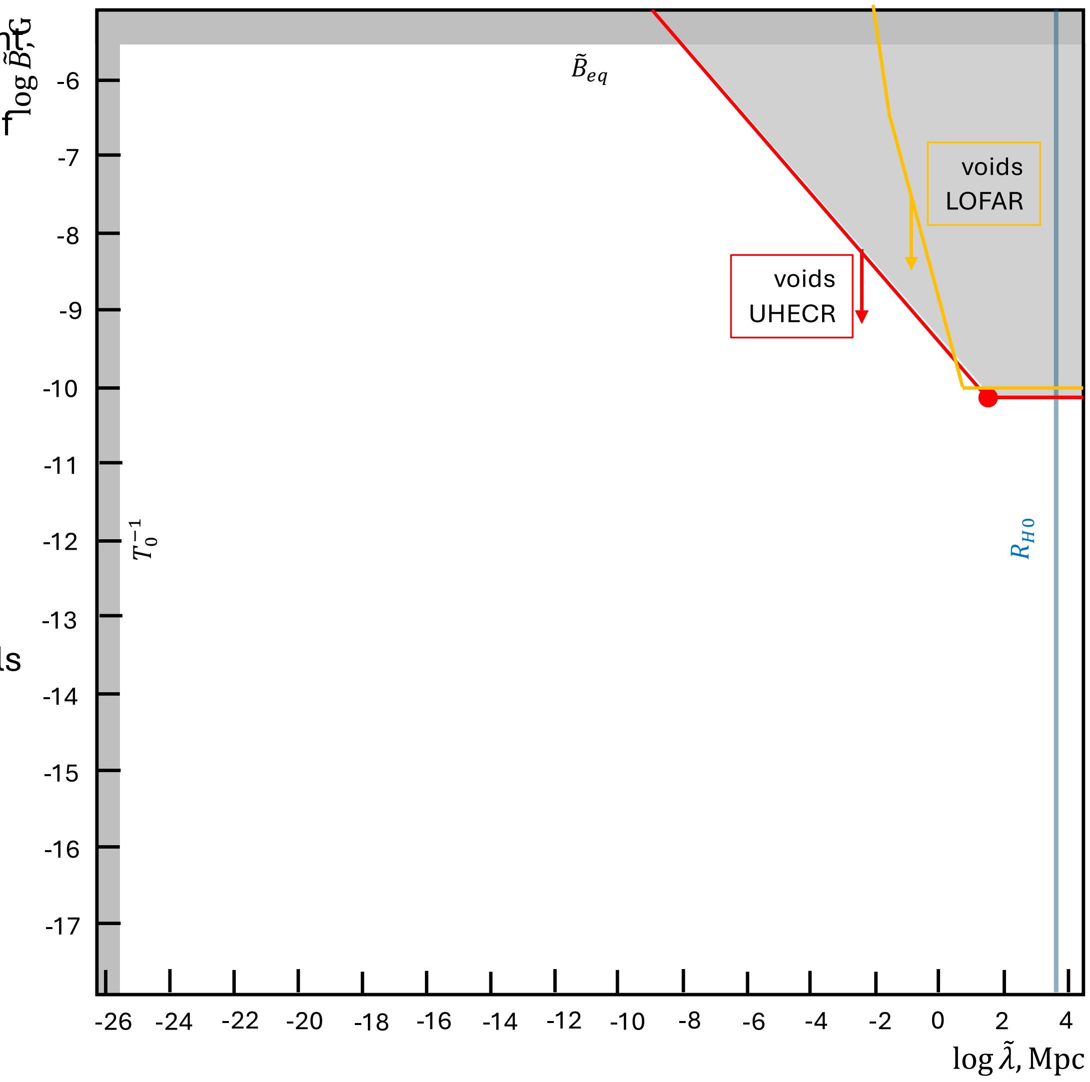

Sensitivity limit of void magnetic field measurements from UHECR

The sensitivity of UHECR technique is about to improve: both existing UHECR experiments (Telescope Array and Pierre Auger Observatory) are upgraded: TAx4 will increase collection area (i.e. get higher UHECR event statistics), Auger Prime will include additional instrumentaiton to measure particle IDs of UHECR (distinguish protons from heavier nuclei).

Detection of a single well-localised proton source within $\delta\theta \simeq 1^\circ$ angular precision of the experiments would constrain the void field down to 10^{-11} G:

$$\theta_{IGMF} = \frac{eBD}{E} \simeq \mathbf{1.5}^\circ \left[\frac{B}{\mathbf{10^{-11}}\ \mathrm{G}}\right] \left[\frac{E}{2.5\times 10^{19}\ \mathrm{eV}}\right]^{-1} \left[\frac{D}{70\ \mathrm{Mpc}}\right]$$

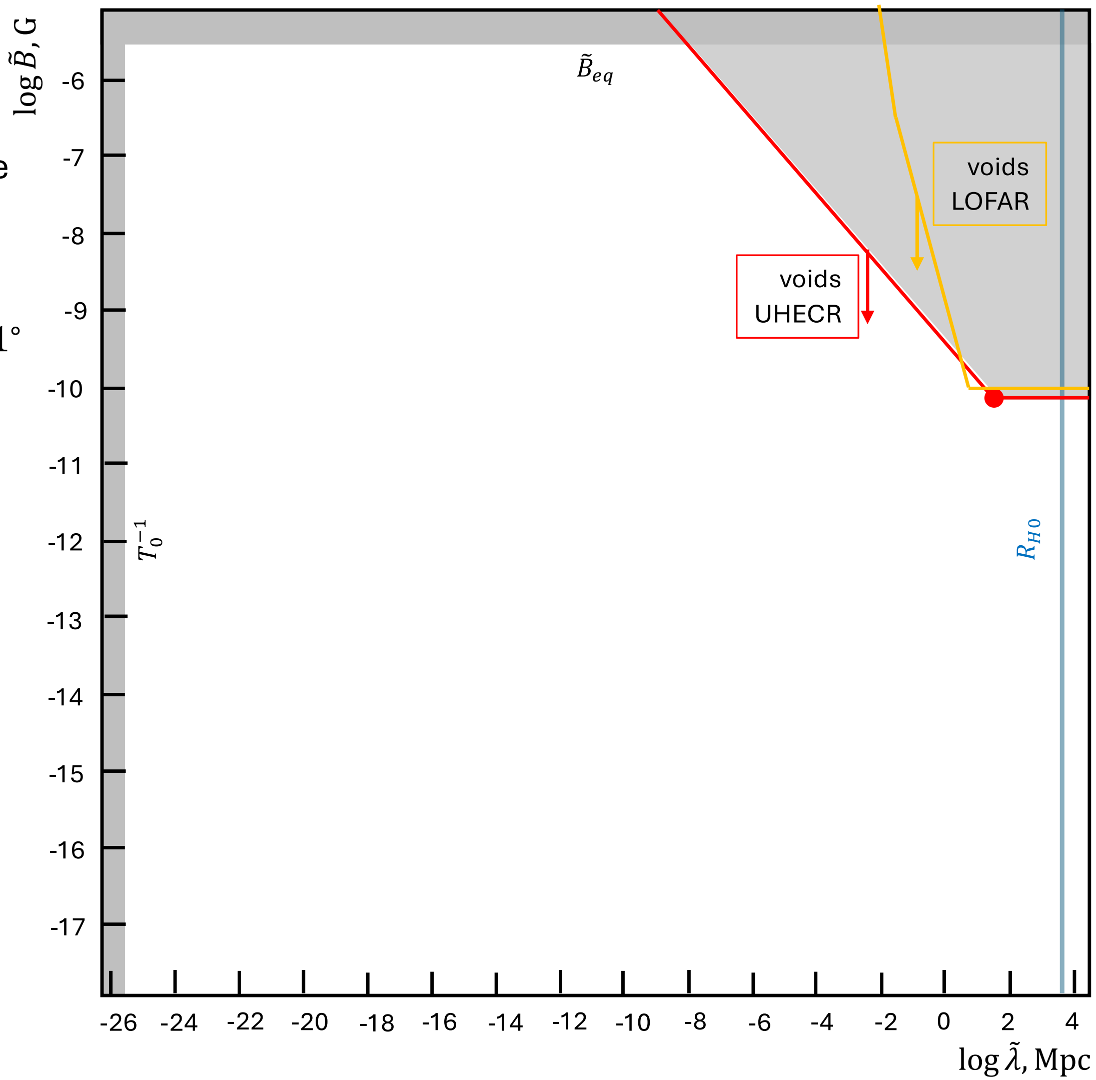

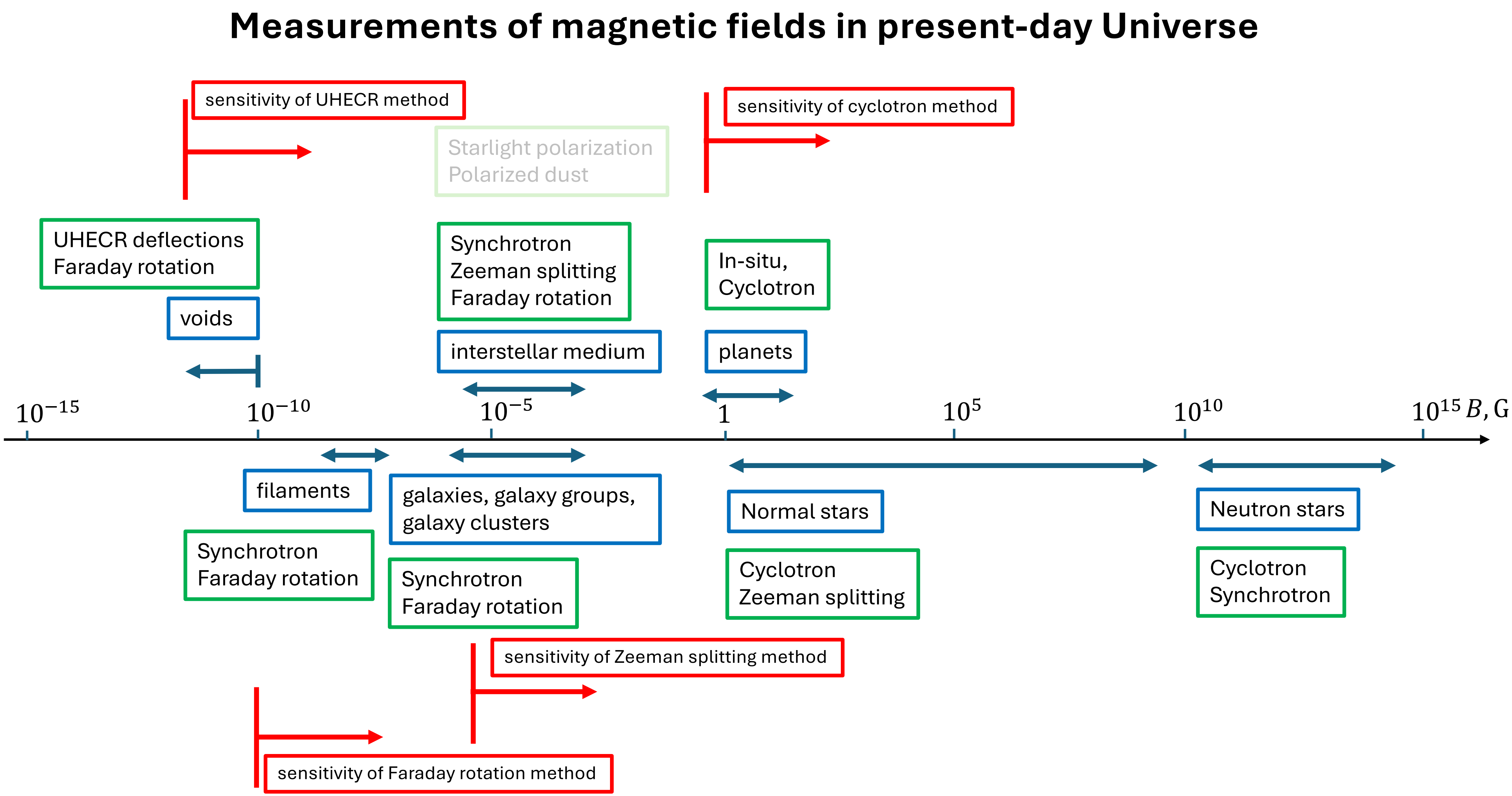
Measurements of magnetic fields in present-day Universe
sensitivity of UHECR method
sensitivity of cyclotron method
Starlight polarization
Polarized dust
UHECR deflections
Faraday rotation
voids
Synchrotron
Zeeman splitting
Faraday rotation
interstellar medium
In-situ,
Cyclotron
planets
10^{-15}
10^{-10}
10^{-5}
1
10^{5}
10^{10}
10^{15} B, G
filaments
galaxies, galaxy groups,
galaxy clusters
Normal stars
Neutron stars
Synchrotron
Faraday rotation
Synchrotron
Faraday rotation
Cyclotron
Zeeman splitting
Cyclotron
Synchrotron
sensitivity of Zeeman splitting method
sensitivity of Faraday rotation method

Gamma-ray interactions in the intergalactic medium

Similar to UHECR, gamma-rays travelling through intergalactic medium start to interact producing secondary particles, if their energy is high enough.

Consider e.g. head-on collisions with low energy photons (of CMB or Extragalactic Backgorund Light, EBL, the cumulative starlight from all galaxies). 4-momenta:

$$P_\gamma = (E, E, 0,0)$$
$$P_{ph} = (\epsilon, -\epsilon, 0,0)$$

Total 4-momentum $P_{tot} = P_{uhecr} + P_{ph}, P_{tot}^2 = -(E+\epsilon)^2 + (E-\epsilon)^2 = -4\epsilon E$.

At the energy threshold of e^+e^- pair produciton, the electron and positron are at rest in the center-of-mass frame, so that in this frame the total 4-momentum is $P_{tot,CM} = (2m_e, 0,0,0), P_{tot,CM}^2 = (2m_e)^2$. The square of the total 4-momentum is a scalar, $P_{tot} = P_{tot,CM}$. This gives

$$E_{thr,e^+e^-} \simeq \frac{m_e^2}{\epsilon} \simeq 2.5\times 10^{11} \left[\frac{\epsilon}{1 \text{ eV}}\right]^{-1} \text{eV}$$

Gamma-rays with energies in the TeV range interact with visible light photons of EBL, gamma-rays with 10^{15} eV energy interact with CMB.

Interactions with EBL lead to suppression of gamma-ray flux on distance scale

$$\lambda_{\gamma\gamma} = \frac{1}{\kappa \sigma n_{ph}}$$

where $\sigma \simeq 10^{-25} \text{ cm}^3$ is the interaction cross-section of e^+e^- pair production.

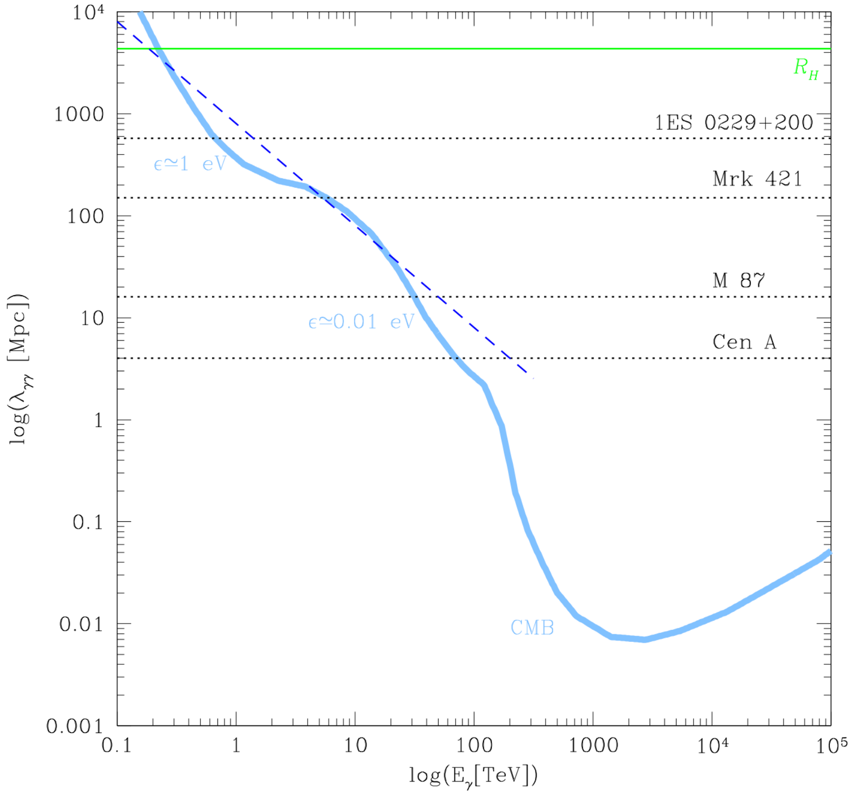

Inverse Compton scattering

Consider an electron in the electric field $E = E_0 \sin \omega t$ of electromagnetic wave. Acceleration $a = eE/m_e$. Dipole radiation intensity, time averaged

$$\langle I \rangle = \frac{2}{3} e^2 a^2 = \frac{2}{3} e^4 \langle E^2 \rangle = \frac{1}{3} e^4 E_0^2 = \frac{4}{3} \sigma_T U_{rad}, \qquad \sigma_T = \frac{8\pi}{3} \frac{e^4}{m_e^2}$$

for non-relativistic electron motion. U_{rad} is the energy density of electromagnetic wave. The radiation can be represented as elastic scattering of photons off electron.

To find the intensity of radiation scattered off relativistic electrons, one can go into reference frame co-moving with electron, use the above formula and do Lorentz transformation back into lab frame. This gives the energy of scattered photons

$$E_\gamma \simeq \gamma^2 \epsilon \simeq 4\times 10^9 \left[\frac{\epsilon}{10^{-3}\ \mathrm{eV}}\right] \left[\frac{E_e}{10^{12}}\right]^2 \mathrm{eV}$$

where ϵ is the initial photon energy and γ the the gamma factor of electron. Scattering off high-energy electrons boosts photon energy and can propulse photons into gamma-ray band.

The intensity of radiation is

$$I = \frac{4}{3} \sigma_T U_{rad} \gamma^2,$$

It scales with particle energy in the same way as synchrotron. The ratio of synchrotron and inverse Compton intensities is

$$\frac{I_{synch}}{I_{IC}} = \frac{U_B}{U_{rad}}$$

Electrons loose energy on inverse Compton scattering over the distance scale

$$D_{IC} = \frac{E}{I} = \frac{3 m_e^2}{4 \sigma_T U_{rad} E} \simeq 100 \left[\frac{U_{rad}}{1 \frac{\mathrm{eV}}{\mathrm{cm}^3}}\right]^{-1} \left[\frac{E}{10^{12}\ \mathrm{eV}}\right]^{-1} \mathrm{kpc}$$

Pair production + Inverse Compton scattering + magnetic field

Combining the two processes, one finds that interactions of TeV gamma-rays with EBL photons are followed by the inverse Compton scatteding of more abundant CMB photons.

If electrons and positrons are not deflected by magnetic fields, the secondary inverse Compton photons are going in almost the same direction as the primary gamma-rays, within an angle

$$\theta \sim \frac{1}{\gamma} = \frac{m_e}{E} \simeq 3\times10^{-5} \left[\frac{E}{10^{12}\ \mathrm{eV}}\right]^{-1} \mathrm{deg}$$

Magnetic field present along the path of gamma-rays deflects electrons and positrons by an angle

$$\Theta = \frac{D_{IC}}{R_L} = \frac{eBD_{IC}}{E}$$

The directions of secondary inverse Compton gamma-rays are not the same as those of the primary gamma-rays.

The secondary signal is detectable as extended emission next to the primary point source and can be used to infer presence of magnetic field along the path of the primary gamma-ray beam.

If the primary source is transient, the secondary signal will arrive with a time delay with respect to the primary source signal.

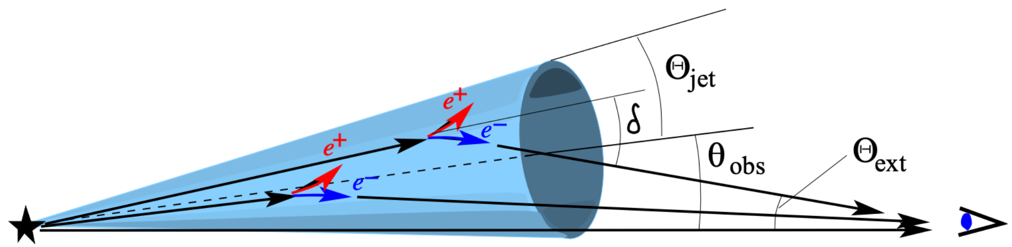

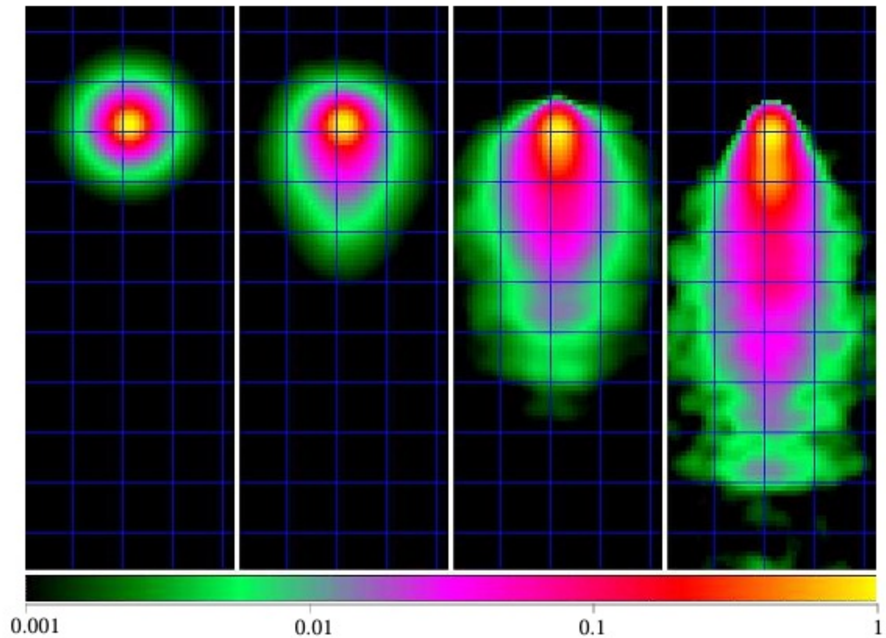

Lower bound on void magnetic fields from gamma-rays

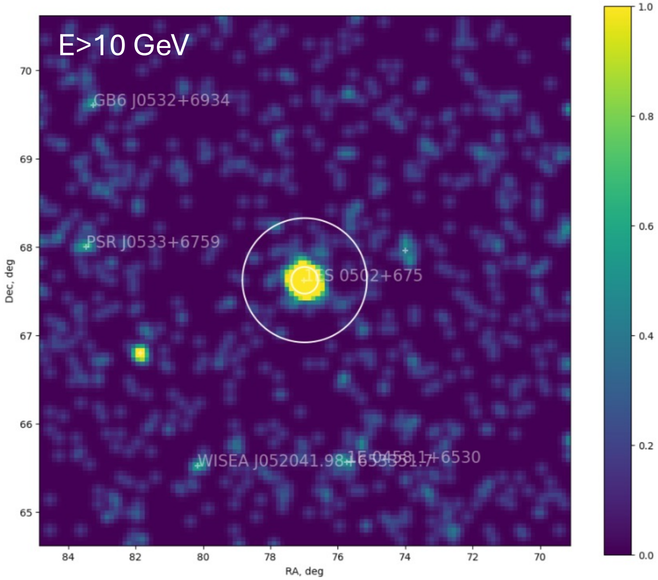

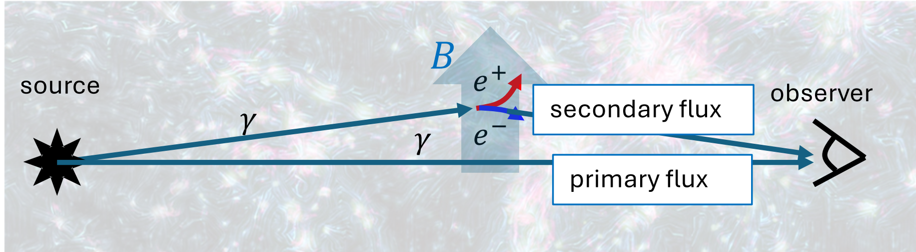

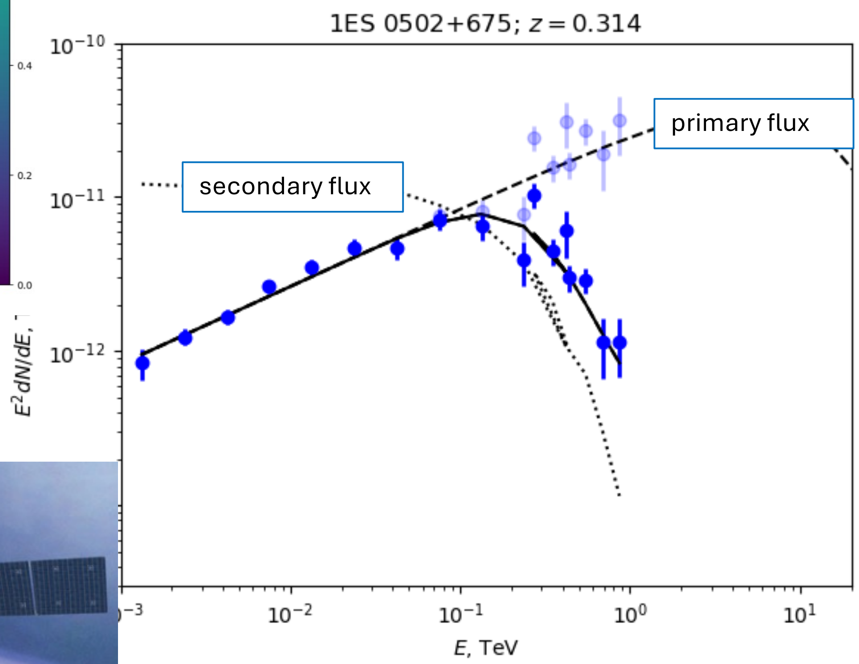

GeV domain: Fermi/LAT

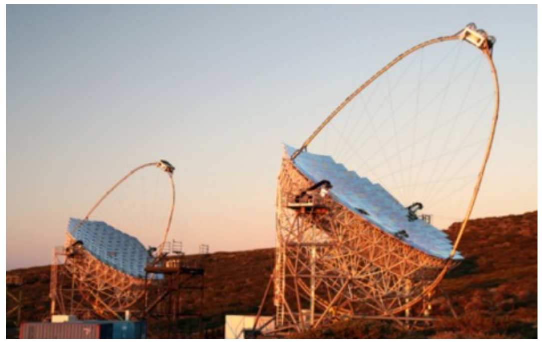

TeV domain: Imaging Atmospheric Cherenkov Telescopes (IACT)

TeV γ-rays from extragalactic sources (active galactic nuclei) deposit pairs in intergalactic medium. Pairs produce secondary γ-rays. Properties of the secondary signal are sensitive to magnetic field in the intergalactic medium.

AN, Vovk 1006.3504; Blunier, AN, Semikoz, 2506.22285

Lower bound on void magnetic fields from gamma-rays

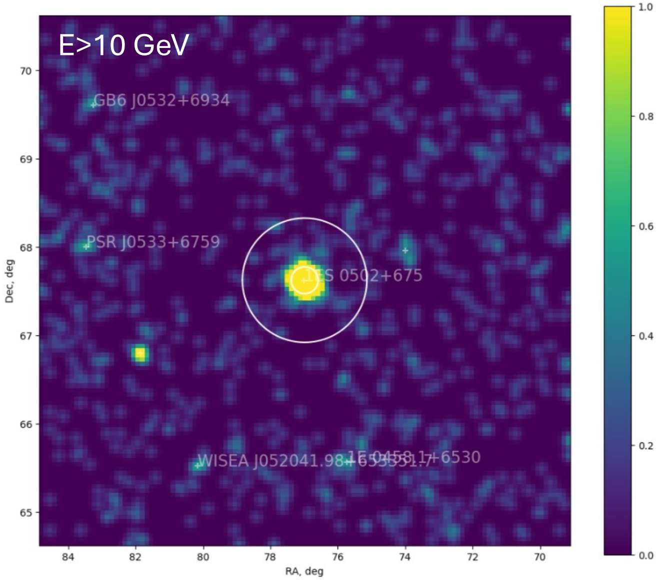

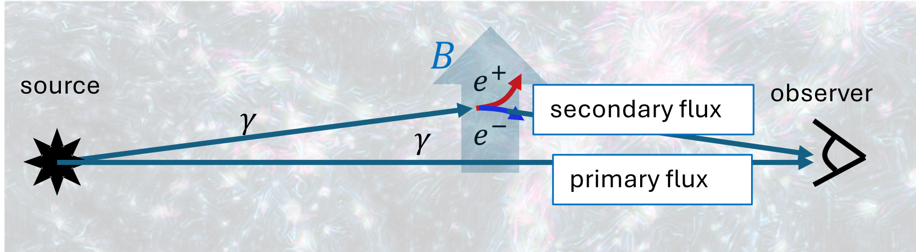

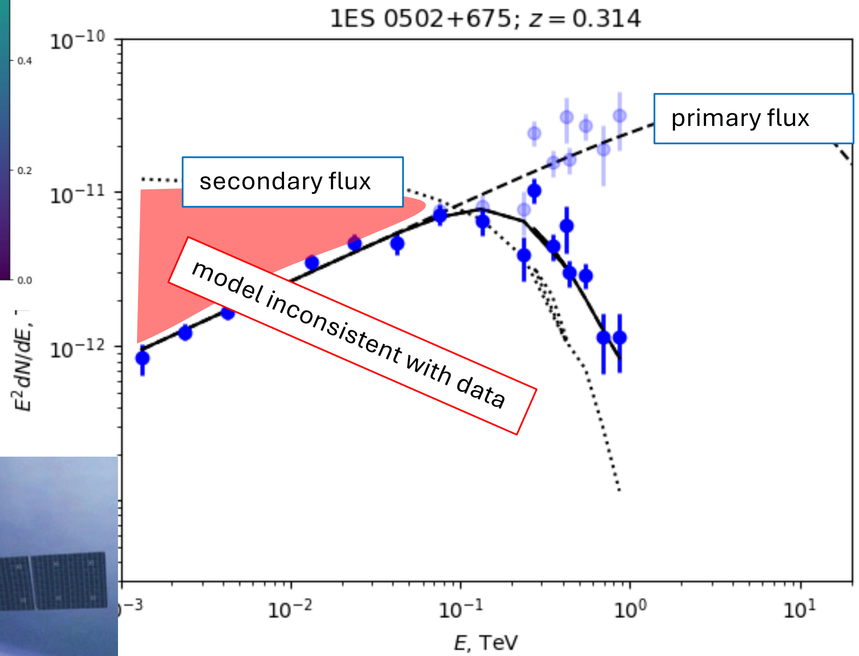

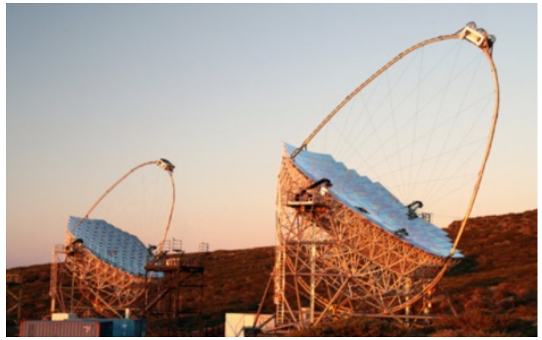

TeV domain: Imaging Atmospheric Cherenkov Telescopes (IACT)

GeV domain: Fermi/LAT

TeV γ-rays from extragalactic sources (active galactic nuclei) deposit pairs in intergalactic medium. Pairs produce secondary γ-rays. Properties of the secondary signal are sensitive to magnetic field in the intergalactic medium.

AN, Vovk 1006.3504; Blunier, AN, Semikoz, 2506.22285

Lower bound on void magnetic fields from gamma-rays

If magnetic field correlation length is $\lambda_B \gg D_{IC}$ electrons are always deflected in the same direction all along their cooling distance with respect to the inverse Compton loss,

$$D_{IC} = \frac{E}{I} = \frac{3m_e^2}{4\sigma_T U_{rad} E} \simeq 100 \left[\frac{U_{rad}}{1\frac{\text{eV}}{\text{cm}^3}}\right]^{-1} \left[\frac{E}{10^{12}\text{ eV}}\right]^{-1} \text{kpc}$$

Otherwise, if $\lambda_B \ll D_{IC}$, electron is only deflected by an angle

$$\delta\Theta = \frac{\lambda_B}{R_L}$$

at each passage of the distance λ_B. Overall, the cooling distance includes $N = D_{IC}/\lambda_B$ parts and deflection direction is randomly changing in different parts, so that the overall deflection angle only grows as

$$\Theta = \sqrt{N}\delta\Theta \propto \lambda_B^{\frac{1}{2}} D_{IC}^{\frac{1}{2}}$$

This explains the change of slope of the lower bound at $D_{IC} = \lambda_B$.

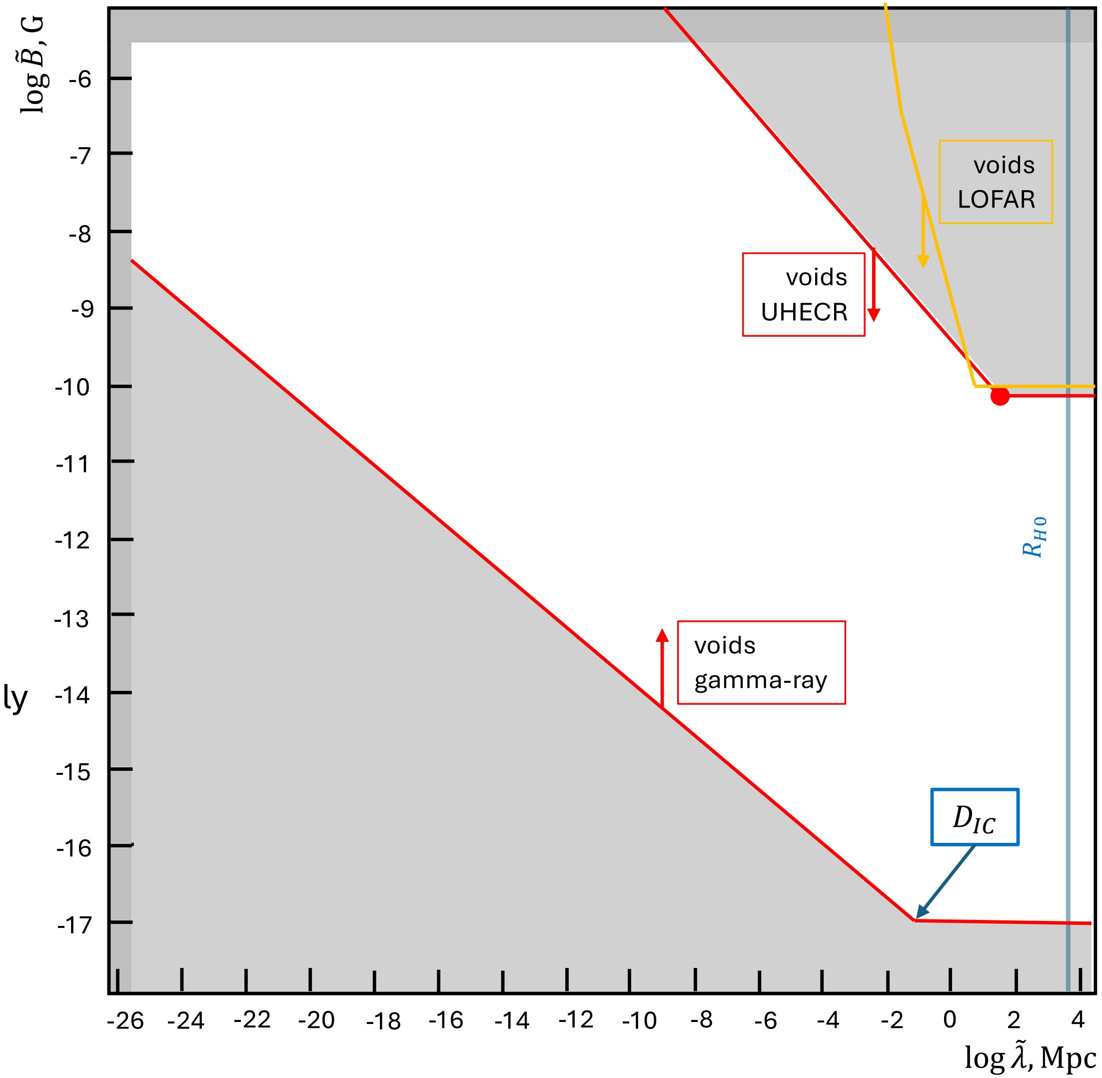

Lower bound on void magnetic fields from gamma-rays

The secondary signal may be absent because the gamma-ray source is transient and the time delay is much longer than the duration of the transient activity of the source.

The "conservative" lower bound shown on the right adopts an assumption that the source (an AGN named 1ES 0502+675) has only "switched on" in gamma-rays at the moment when telescopes started to observe it (~ 20 yr ago).

This assumption is most probably not valid: the duty cycle of AGN activity is estimated at $\sim 10^7..10^8$ yr. However, transient gamma-ray activity of AGN has also been observed and the possibility that one specific source is transient cannot be ruled out.

... the possibility that a set of ~ 10 AGN selected for the analysis of Blunier, AN, Semikoz, 2506.22285 includes only transients all of which only started their activity 20 years ago is unlikely...

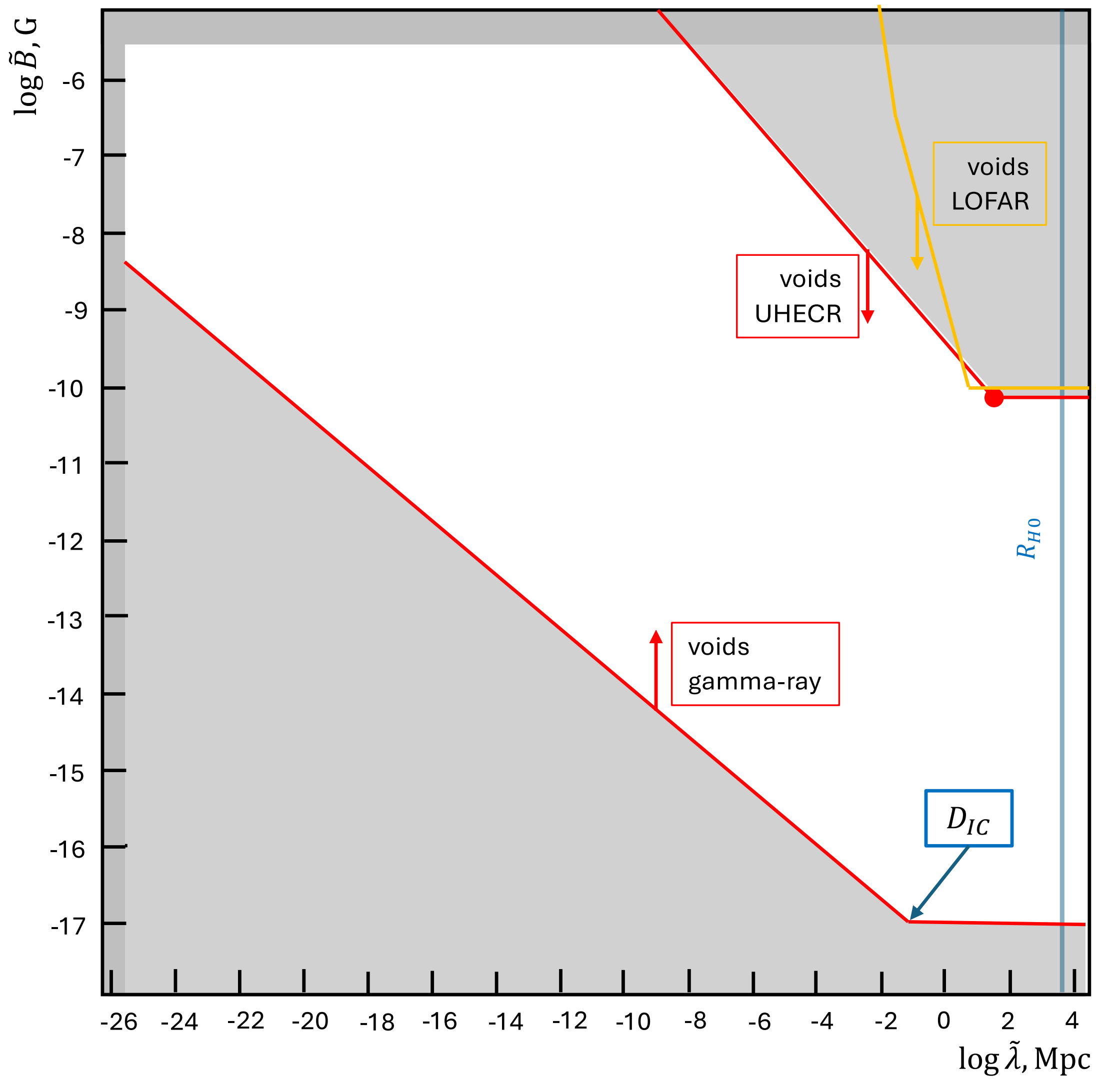

Measurement of void magnetic fields using gamma-rays

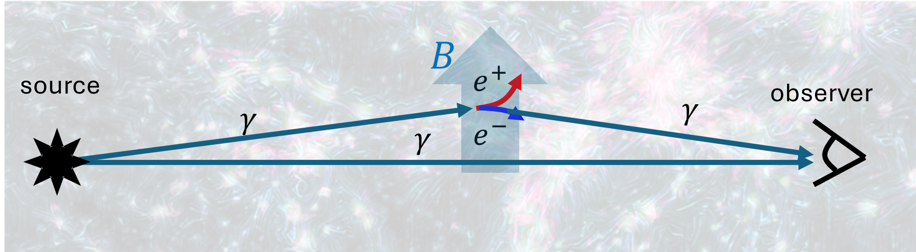

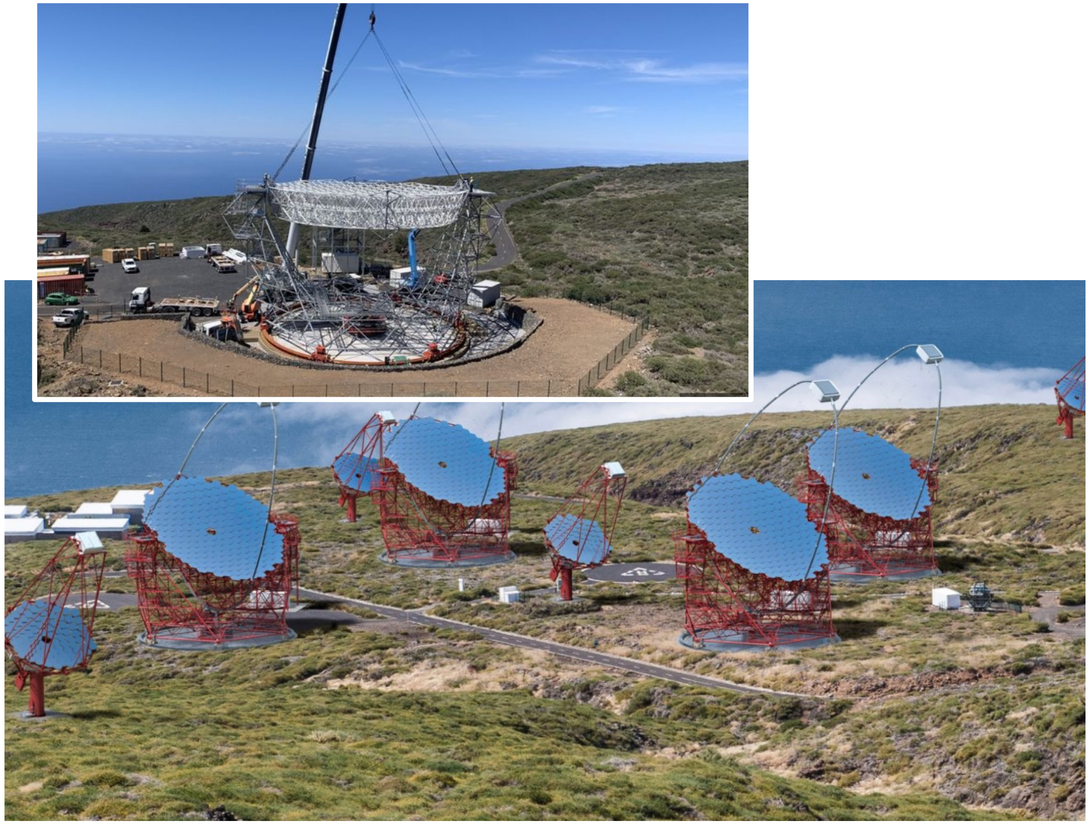

Cherenkov Telescope Array Observatory (CTAO)
... in construction, complete by 2028

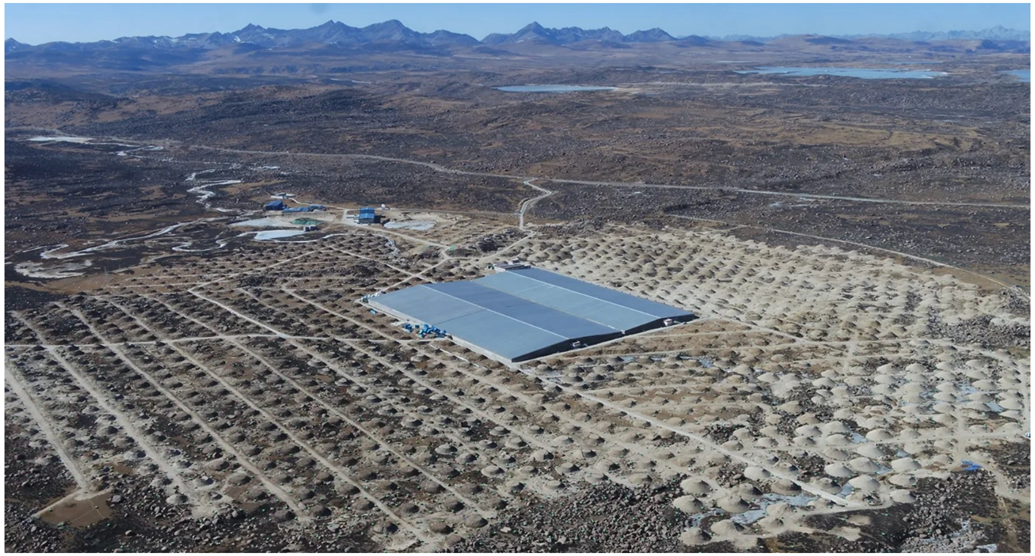

Large High-Altitude Air Shower Observatory (LHAASO)
.... taking data since ~3 years

Lower bound on void magnetic fields from gamma-rays

Sensitivity boost provided by new generation of gamma-ray telescopes enables measurement of void magnetic field via detection of extended emission around AGN or delayed emission from Gamma-Ray Bursts, if the IGMF parameters are within the hatched region.

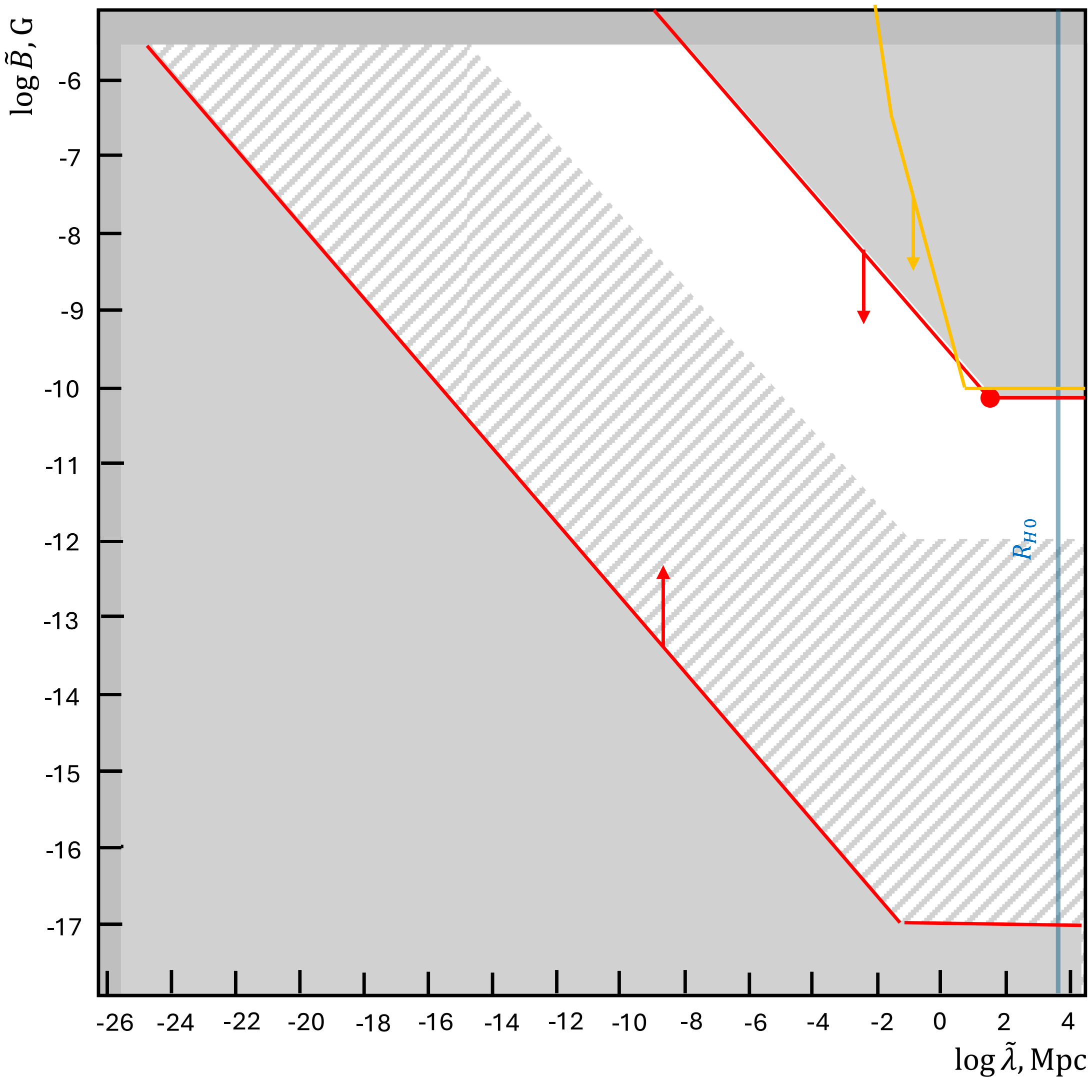

Constraint on magnetic field correlation length

Comoving magnetic field evolution is guided by the induction on largest distance scales by the induction equation

$$\partial_{\tilde{t}}\tilde{B} \simeq \nabla\times(\vec{v}\times\tilde{B})$$

The time scale of field transformation on distance scale $\tilde{L}$ can be estimated from order-of-magnitude version of this equaiton

$$\frac{\tilde{B}}{\tilde{t}} \sim \frac{v\tilde{B}}{\tilde{L}}, \qquad \tilde{t} \sim \frac{\tilde{L}}{v}$$

Maximal scale of fields that can be transformed in the course of evolution of the Universe is $L_{ple} \sim vt_H = vH_0^{-1}$. The velocity scale of reference in Magneto-Hydro-Dynamics is Alfven velocity at which the kinetic energy density of plasma motions is comparable to the energy density of magnetic field driving these motions

$$\frac{\rho v_A^2}{2} = \frac{B^2}{8\pi}, \qquad v_A = \frac{B}{\sqrt{4\pi\rho}}$$

Taking $v = Cv_A$ (C is a numerical factor), one finds that the largest distance scale affected by evolution is

$$L_{lpe} \sim C\frac{BH_0^{-1}}{\sqrt{4\pi\rho_b}}$$

where $\rho_b = \Omega_b\rho$ is the density of baryonic matter. Estimating

$$\rho = \frac{3M_{Pl}^2H_0^2}{8\pi}$$

From Friedman equation, one finds

$$L_{lpe} \sim C\frac{BH_0^{-1}}{\sqrt{\Omega_b M_{Pl}^2 H_0^2}} = \frac{B}{\Omega_b^{\frac{1}{2}} M_{Pl} H_0^2} \simeq 1\, C\left[\frac{B}{10^{-8}\ \mathrm{G}}\right]\ \mathrm{Mpc}$$

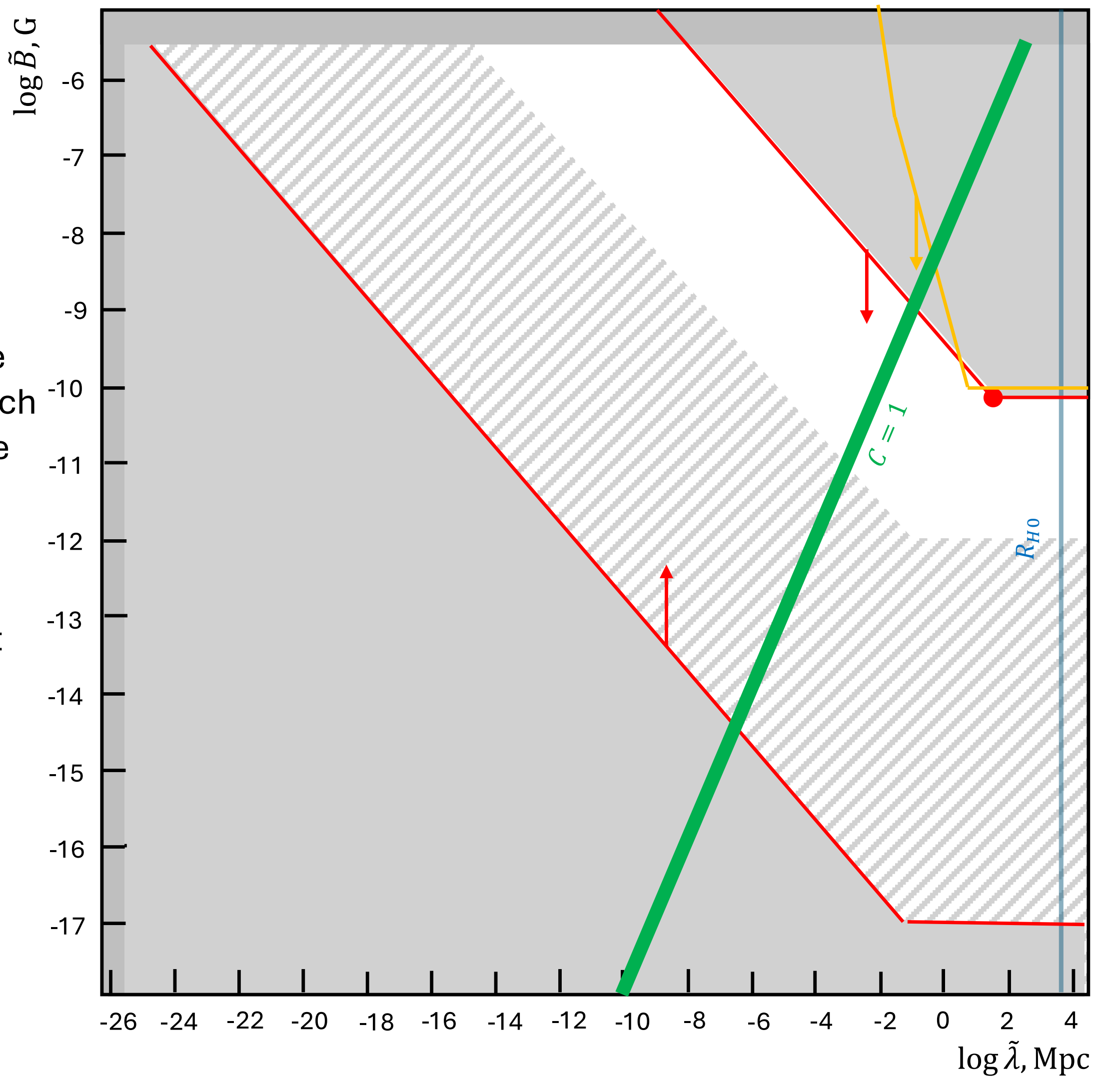

Constraint on magnetic field correlation length

$$L_{lpe} \sim C \frac{B H_0^{-1}}{\sqrt{\Omega_b M_{Pl}^2 H_0^2}} = \frac{B}{\Omega_b^{\frac{1}{2}} M_{Pl} H_0^2} \simeq 1\, C \left[\frac{B}{10^{-8}\ \mathrm{G}}\right] \mathrm{Mpc}$$

The value of the factor C is debated, $C \sim 10^{-2}$ has been found in numerical studies (see lectures A.Brandenburg).

Magnetic fields in in the voids that are variable on shorter distance scales should have decayed due to development of turbulence by now. One generically expects that only fields variable on scales larger or comparable to L_{lpe}, within the extent of blue-shaded region, should be present in the voids.

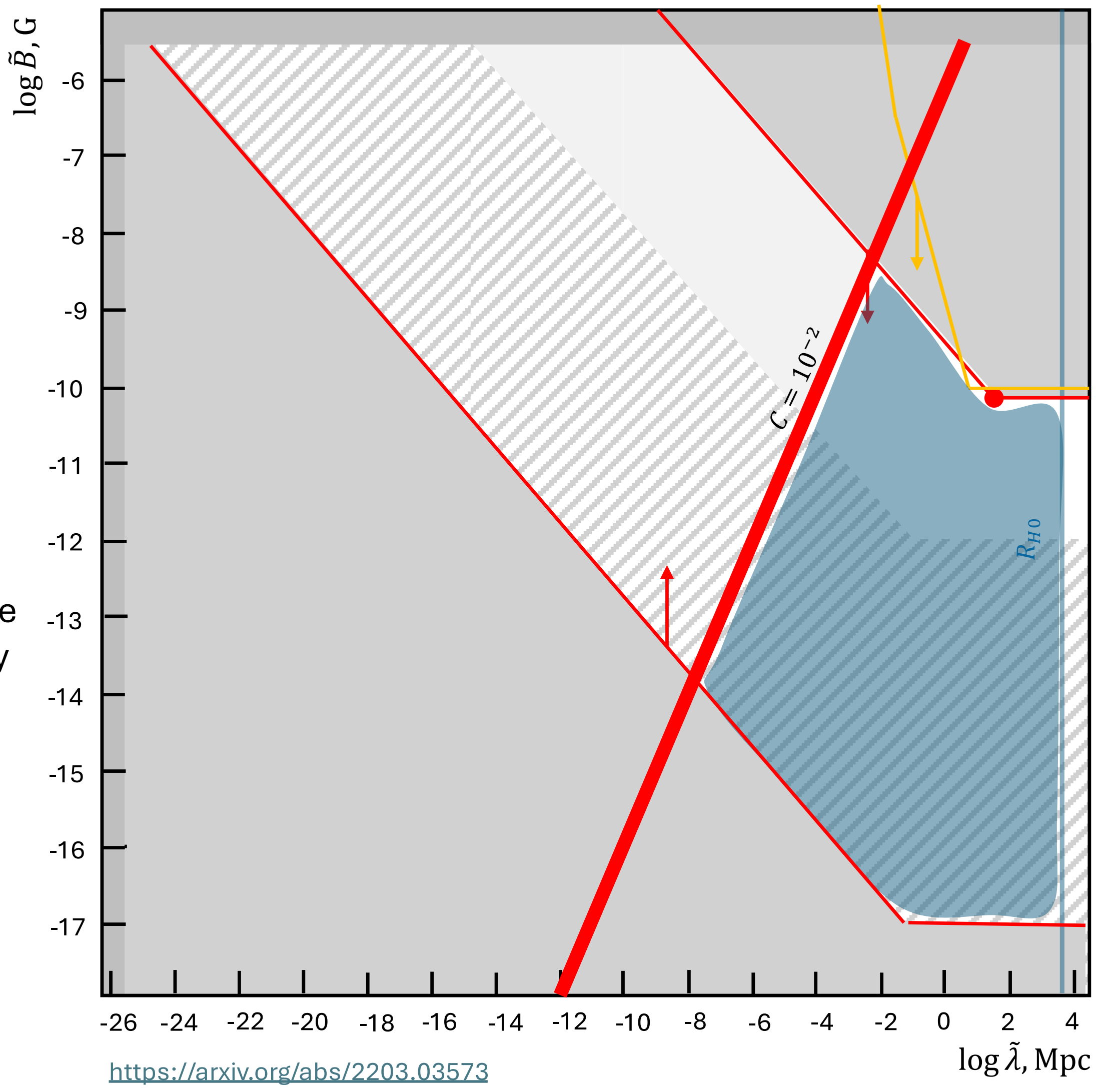

https://arxiv.org/abs/2203.03573
https://arxiv.org/abs/2401.08569

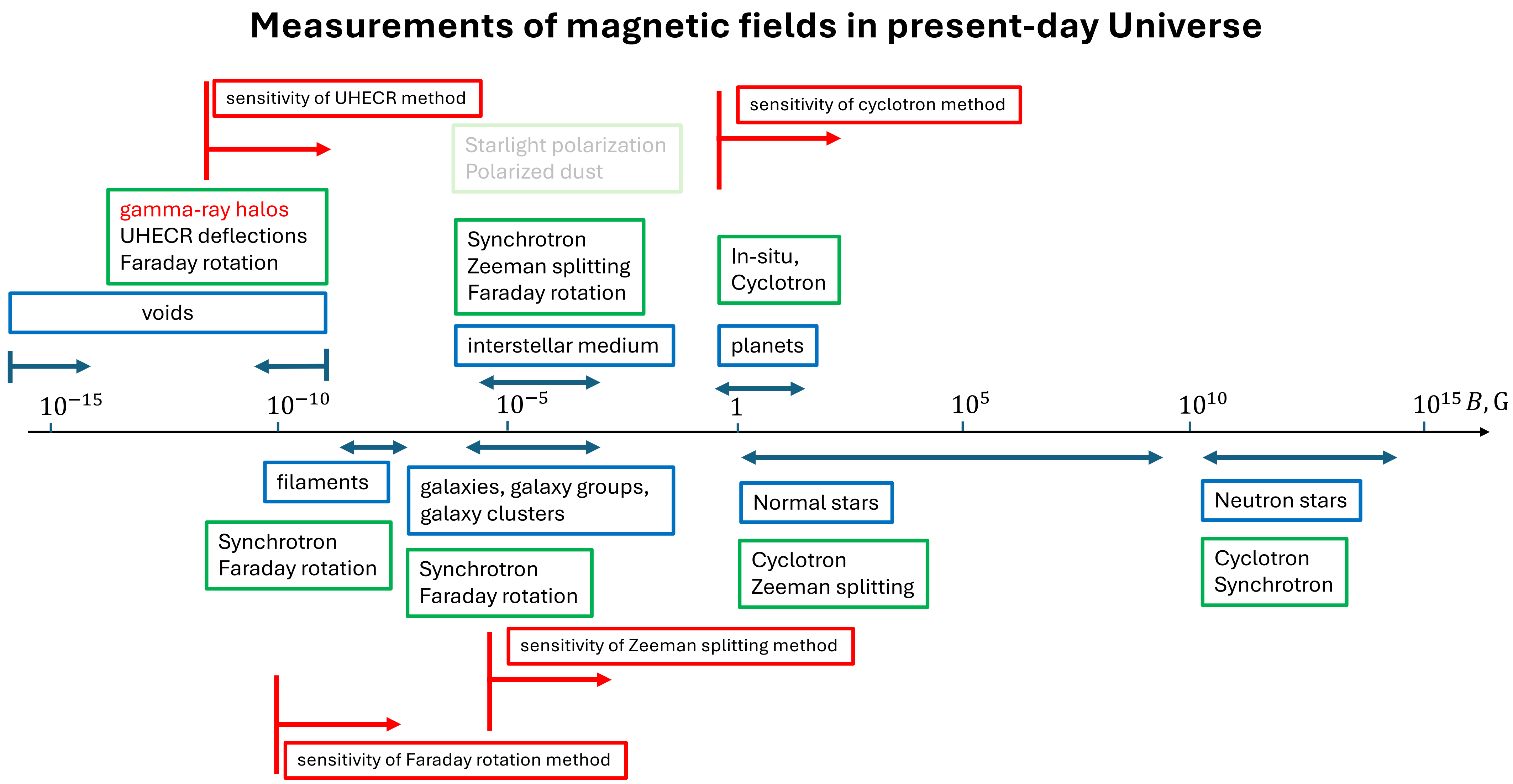

Measurements of magnetic fields in present-day Universe
sensitivity of UHECR method
sensitivity of cyclotron method
Starlight polarization
Polarized dust
gamma-ray halos
UHECR deflections
Faraday rotation
voids
Synchrotron
Zeeman splitting
Faraday rotation
interstellar medium
In-situ,
Cyclotron
planets
10^−15
10^−10
10^−5
1
10^5
10^10
10^15 B, G
filaments
Synchrotron
Faraday rotation
galaxies, galaxy groups,
galaxy clusters
Synchrotron
Faraday rotation
Normal stars
Cyclotron
Zeeman splitting
Neutron stars
Cyclotron
Synchrotron
sensitivity of Zeeman splitting method
sensitivity of Faraday rotation method

Constraint on magnetic field correlation length

The notion of the "largest processed eddies" can be introduced for any moment in the history of the Universe. $\tilde{L}_{ple} \sim v\tilde{t}_H$
where $v = Cv_A$ and

$$v_A = \frac{B}{\sqrt{4\pi\rho}}$$

The density ρ in the denominator is the total density of species coupled to the charged particle plasma. For example, at the epoch of QCD phase transition, plasma of charged particles is coupled to photon, and neutrino fluid. In this case,

$$\tilde{L}_{lpe} \sim C\tilde{R}_H\left(\frac{\tilde{B}}{\tilde{B}_{eq}}\right)$$

In the absence of field forcing of magnetic field at specific distance scale during the epoch of interest, all the field modes with wavelengths shorter than L_{lpe} would have decayed due to development of turbulence and the magnetic field of strength $\tilde{B}$ is supposed to have the correlation length $\tilde{L}_{lpe}$.

The largest processed eddy line slides toward larger correlation lengths in the course of the Universe history, sweeping a plane through $t, \tilde{B}, \tilde{\lambda}_B$ parameter space (see 3d model).